

ORIGINAL ARTICLE

Aedeagus evolution promotes speciation? A primary pattern in rove beetle phylogeny

Xi Zhang^{1, 2, 3}, Hongzhang Zhou^{1, 2 *}

¹Key Laboratory of Zoological Systematics and Evolution, Institute of Zoology, Chinese Academy of Sciences, Beijing 100101, China

²University of the Chinese Academy of Sciences, Beijing 100049, China

³Department of Parasitology, Medical College, Zhengzhou University, Zhengzhou 450052, China

*Corresponding author, E-mail: zhouhz@ioz.ac.cn

Abstract Global species diversity is a historical result of speciation minus extinction and can be exhibited by phylogenetic patterns, whereas speciation is a process that may concern reproductive isolation and relating, at least in most sexual reproductive insects or other similar animals, to genital morphological evolution. The aedeagus is male genital organ that determines valid mating and reproductive isolation. However, definite correlation between aedeagus variation and species richness has not yet been clearly demonstrated. Here the phylogenetic tree of the rove beetle subfamily Staphylininae is built up based on 3085 bp DNA sequences of cytochrome oxidase subunit I (COI), nuclear 28S rDNA, nuclear genes wingless (Wg) and topoisomerase I (TP). Branching times and confidence intervals are calculated with molecular clock calibrations based on rove beetle fossil records. Different types of aedeagus, namely, median lobe plus a single paramere (Asp), a pair of parameres (App), or a single but bifurcated paramere (Abp), are marked on the phylogenetic tree and the genital morphological variations are compared in different genus-level taxa. The result shows that active cladogeneses occurred during late Cretaceous to late Paleogene, with those clades of Staphylininae evolved to be a more species-rich ones accompanied by larger aedeagus modifications. This implies that male genital morphological evolution might promote rove beetle speciation.

Key words Beetle phylogeny, Staphylininae, aedeagus, species richness.

1 Introduction

Beetles comprise at least one fourth of all species on the earth and thus represent the most diversified and successful lineage of all organisms (Bouchard *et al.*, 2009; Lawrence *et al.*, 2011; Simmons & Smith, 2011). Why are there so many beetles? This question has fascinated evolutionary biologists for a long time (Crowson, 1960; Farrell, 1998; Grove & Stork, 2000; Hunt *et al.*, 2007). During the last two decades, many excellent advances were made in recognizing the large-scale patterns of beetle species diversity (Farrell, 1998; Engel & Roff, 1990; Wilf *et al.*, 2000; Grimaldi, 2004; Hunt *et al.*, 2007; Sota & Nagata, 2008; Lawrence *et al.*, 2011; Ikeda *et al.*, 2012). Some pioneer scientists concentrated their studies on recognizing the extraordinary diversity of phytophagous beetles and excellent progress was achieved (Farrell, 1998; Wilf *et al.*, 2000; Novotny *et al.*, 2006; Gómez-Zurita *et al.*, 2007; Janson *et al.*, 2008; Winkler *et al.*, 2009). However, our knowledge of the diversity of non-phytophagous beetles is still fragmentary and we are far from a comprehensive view of the large-scale patterns of beetle species diversity in total.

urn:lsid:zoobank.org:pub:355DC1A6-011E-4A31-B6CA-CD57A1CF8947

Received 2 May 2017, accepted 2 February 2018

Executive editor: Fuqiang Chen

Evolutionary success of a species depends on its survival ability and is closely related to its reproductive capacity and mating success for sexual-reproducing species (Eberhard, 1985). Any morphological changes and variations in reproductive organs that may affect fertilization and breeding success can lead to modifications in species adaptations and eventually the model and rate of speciation (Edwards, 1993; Arnqvist & Danielsson, 1999; Wenninger & Averill, 2006; Matocq *et al.*, 2007). The morphology of male genitalia is found to be more variable among species than other organs; even closely allied species with similar general morphology exhibit frequently striking differences in their genitalia or other reproductive organs (Arnqvist, 1997; Eberhard *et al.*, 1998; Eberhard, 2010; Reinhardt, 2010). As a matter of fact, taxonomists identify species mostly according to the differences exhibited in genitalia morphology and/or other characteristics of reproductive organs (Arnqvist, 1998). Many hypotheses were proposed to explain this phenomenon, such as sexual selection, which was put forward as the major explanation of genital variation and complexity, as well as the related mechanism of speciation as the most potent force in driving reproductive isolation. This notion arose from observations that species differ, to the most extent, in those traits involved with mating success and was supported by models of sexual selection-driven speciation (Hosken & Stockley, 2004; Mendez & Aguilar, 2004; House & Simmons, 2005; Ritchie, 2007; Reinhardt, 2010). Therefore, the morphological variations of genitalia or other reproductive organs may be important to understand how they would be evolved and what kind of influence they had in speciation and diversification. More attention should be paid to these variations to unravel the fundamentals of beetle diversity and speciation. Although many studies focused on genitalia morphology and reproductive success, few provided a definite relationship between genital morphological changes and species richness. In this paper, we try to demonstrate a correlation between how large the scope of aedeagus variation and how many species of a rove beetle clade.

In this study, we selected the rove beetle subfamily Staphylininae (Coleoptera: Staphylinidae) as suitable representative taxon. Firstly, the subfamily Staphylininae is a species-rich group with life style as predators and very high biological diversity in the view of global scale; it can be considered as one of the most successful groups of organisms that is well-adapted to different types of habitats (Newton & Thayer, 1992; Grebennikov & Newton, 2009; Chatzimanolis *et al.*, 2010). Secondly, the modern taxonomic system of this subfamily was evaluated phylogenetically based on adult and larval morphology and molecular data (Solodovnikov & Newton, 2005; Chatzimanolis *et al.*, 2010; Zhang & Zhou, 2013). Thus, this group can be considered as a suitable one in order to recognize new biological patterns (if any) and to unravel the large sample data of DNA sequences and morphological measurements. We focused on the following problems: (1) construct phylogenetic trees with high level of confidence and molecular clock calibration based on rove beetle fossil records; (2) recognizing morphologically the different types of aedeagus (exactly, structures and configurations of median lobe and paramere), and marking them on the best-fitted phylogenetic tree; (3) plotting the genital morphological variations (types and paramere/aedeagus length ratios) to the species numbers of different genus-level taxa.

2 Materials and methods

2.1 Taxon selection and sampling

A total of 58 species belonging to 48 genera representing six of all seven tribes of Staphylininae were included in this study (Supplementary Table S1). The tribe Staphylinini is the very large one represented by 41 species 36 genera; many valuable DNA sequence data were from the data set of Chatzimanolis *et al.* (2010). The tribe Xantholinini was represented by 12 species 7 genera. The presumably close subfamilies Omaliinae and Oxyporinae (Grebennikov & Newton, 2009) were included as outgroup to root the resulting trees.

2.2 DNA extraction, amplification and sequencing

DNA was extracted from head and prothorax of beetles using Tiangen DNeasy Blood and Tissue Kit (Tiangen, China) following the manufacturer's protocol. Four target genes were amplified by PCR using the primer combinations listed in the supplementary material table S2: the mitochondrial cytochrome oxidase subunit I (COI), the nuclear protein-coding wingless (Wg), the nuclear protein-coding topoisomerase I (TP), and a portion of the ribosomal 28S rDNA (28S) sequence. PCR amplification was fulfilled following the protocols as described in Chatzimanolis *et al.* (2010). PCR products were purified using High Pure PCR Product Purification Kit (TAKARA BIO INC., China) and sequenced in both directions using the automated sequencer (ABI Prism 3730 XL DNA Analyzer; ABI Prism, Foster City, CA) in Beijing Genomics Institute.

2.3 Sequence alignment

The sequences for COI, Tp and Wg were initially aligned using the default settings in Clustal X version 2.0 (Higgins *et al.*, 2007) and adjusted in Se-Al v2.0a11 (Rambaut, 2002). For the 28S rDNA sequences, secondary structure was inferred through comparison with published secondary structures of *Tenebrio* sp. (Gillespie *et al.*, 2004) and used as a guide for manual sequence alignment in Mega 5.0 (Tamura *et al.*, 2011).

2.4 Phylogenetic analysis

DNA sequence data of different markers (28S, COI, Tp and Wg) were analyzed in combination, using Bayesian Inference (BI) and Maximum Likelihood (ML) respectively, two phylogenetic inference methods. BI analyses were performed in MrBayes v3.1 (Ronquist & Huelsenbeck, 2003) with 5,000,000 generations, sampling trees every 100 generations. Sequence evolution models were selected using Modeltest 3.7 (Posada & Crandall, 1998) under the Akaike information criterion. Likelihood values were observed with Tracer v1.5 (Rambaut & Drummond, 2007), discarding all the trees before stability in likelihood values as a ‘burn in’ (first 10,000 trees). Stationarity was also reassessed using a convergence diagnostic. An average standard deviation of the split frequencies < 0.03 were used as criteria of convergence between both runs. ML analyses were performed in PhyML (Guindon & Gascuel, 2003) with models selected by Modeltest 3.7 (Posada & Crandall, 1998).

2.5 Divergence time estimation

The concatenated sequence alignment was analyzed with a relaxed molecular-clock model using the Bayesian phylogenetic software BEAST 1.6.1 (Drummond & Rambaut, 2007). The alignment was partitioned into four subsets according to different genes. Each subset was assigned an independent model of nucleotide substitution, chosen using the Modeltest 3.7 (Posada & Crandall, 1998). Rate variation among branches was modeled using uncorrelated lognormal relaxed clocks (Drummond *et al.*, 2006). A Yule process was used for the tree prior. Posterior distributions of the parameters, including the tree, were estimated via Markov chain Monte Carlo (MCMC) sampling. Two replicate MCMC runs were performed, with the tree and parameter values sampled every 1×10^3 steps over a total of 1×10^8 steps. The diagnostic software Tracer 1.5 (Rambaut & Drummond, 2007) was used to assess convergence between runs, to estimate an appropriate number of samples to be discarded as burn-in, and to ensure that effective sample sizes (i.e. > 200) were sufficient to provide reasonable estimates of model parameter variance. Samples from the posterior of both independent runs were combined and the trees and parameter values were summarized. The sampled tree with the maximum product of clade credibilities was identified using TreeAnnotator (Drummond & Rambaut, 2007) and viewed using FigTree 1.3.1 (Rambaut, 2009).

The minimal known ages of subfamilies Omaliinae and Oxyporinae based on fossil records, were used as prior to estimate the divergence time of representative nodes. A normal distribution was used to provide for uncertainties of fossil of all calibration points (Ho, 2007). More specifically, the following two calibration points were used. (1) The subfamily Omaliinae: we used a normally distributed estimate prior of 165 Mya, SD 5.0 (95% interval: 155.2–174.8 Mya) based on the fossil *Prostaphylinus mirus* in the Middle Jurassic Haifanggou Formation from the Haifanggou Village, Beipiao, Liaoning Province, north-east China (Cai & Huang, 2010). (2) The clade Oxyporinae: we used a normally distributed estimate prior with mean value being 127.5 Mya, and SD 5.0 (95% interval: 117.7–137.3 Mya) based on the fossil *Oxyporus yixianus* in the Early Cretaceous Yixian Formation from Chaomidian Village, Beipiao City, Liaoning Province, north-east China (Yue *et al.*, 2011).

2.6 Imitation and measuring of aedeagus

For aedeagus morphology, those aedeagus line drawings or photo figures, either got from our early studies or from the published papers treating the genera we selected, were used here. Aedeagus structures were characterized by using the software Inkscape (Portable edition). Then each imitated aedeagus and corresponding paramere was mapped onto the phylogenetic tree, and pruned to include only the in-group taxa. The length of aedeagus and corresponding paramere for each selected genus was measured using the distance tool of Image Processing Toolbox 7 in the mapping software MatLab v.7.9.0. The species numbers and geographical distributions for those selected genera were based on the catalog of Herman (2001) and other related publications. In order to investigate the evolutionary trend of the aedeagus morphology, we introduced Paramere-to-Median-lobe Index (PM Index): $\text{PM Index} = (\text{median-lobe length} - \text{paramere length}) / \text{median-lobe length}$, so that we were able to plot the scope of aedeagus variations to the clade divergence times.

3 Results

3.1 Phylogenetic relationships

Phylogenetic analyses were based on one nuclear ribosomal (28S = 899–1132 bp) and three protein coding (COI = 792–834 bp, Wg = 366–438 bp, Tp = 600–726 bp) loci. The concatenated sequence alignment contained 61 sequences and 3085 positions after trimming (Table 1). The likelihood models identified by Modeltest (AIC) were given in Table 2. In the Bayesian analysis (Fig. 1), the subfamily Staphylininae was recovered as monophyletic with a high posterior probability support value (pp = 0.99). The tribe Platyprosopini was in the basal of the subfamily Staphylininae. Excluding the tribe Platyprosopini, another five tribes made up two main clades: one clade including the tribes Staphylinini and Arrowinini (Clade A in Fig. 1), the other clade containing Xantholinini, Othiini and Diochini three tribes (Clade B in Fig. 1). In Clade A, several small clades were all with a 1.0 posterior probability support value, including the clades such as Staphylinina + Anisolinina, Xanthopygina, Philonthina and Tanygnathina + Hyptiomina. In Clade B, Xantholinini and Othiini two sub-clades were also well supported (pp = 1.0). The maximum likelihood analysis generated a similar topology as Bayesian analysis except for the placement of the subtribe Amblyopinina and the genus *Algon* (Supplementary Fig. S3).

Table 1. Details on the concatenated alignment of the four target regions used in this study.

	COI_1st	COI_2nd	COI_3rd	Wg_1st	Wg_2nd
No. of taxa	61	61	61	61	61
Excluded positions	3 ^a	3 ^a	3 ^a	10 ^b	10 ^b
Final length	275	275	275	136	136
Constant sites	154	215	11	84	95
Uninformative sites	28	26	12	7	9
Informative sites	93	34	252	45	32
Mean base frequency					
A	30.3	19.5	45.1	33	36.6
C	15.4	23.8	10.3	25.6	20.1
G	24.7	14.9	2.2	24.9	24.4
	Wg_3rd	Tp_1st	Tp_2nd	Tp_3rd	28S
No. of taxa	61	52	52	52	55
Excluded positions	10 ^b	1 ^c	1 ^c	1 ^c	53 ^d
Final length	136	241	241	241	1129
Constant sites	5	144	161	5	448
Uninformative sites	4	24	32	3	244
Informative sites	127	73	48	233	437
Mean base frequency					
A	12.7	34	45.8	22.3	19.8
C	44.4	17.3	16.9	23.1	28.8
G	26.1	32.2	11.5	29.5	33

^aThree codons at the 5' end of COI excluded due to gene length polymorphism

^bThirty positions of Wingless excluded due to ambiguous alignment

^cOne codon at the middle of Tp excluded due to ambiguous alignment

^dPositions excluded due to ambiguous alignment

3.2 Evolutionary trends of paramere morphology and cladogenesis of species-rich groups

According to the relaxed molecular clock analysis of the combined data, the origin of the subfamily Staphylininae was estimated at about 176.11 million years ago (Mya) with a 95% confidence interval from 161.38 Mya to 190.78 Mya. The Beast analysis for the age of important clades, such as Clade A and Clade B, and clades Staphylinina + Anisolinina, Xanthopygina, Philonthina, Tanygnathina + Hyptiomina, Othiini and Xantholinini, were shown in Table 3. Here we selected the Bayesian tree to show the phylogenetic pattern of aedeagus morphology and divergence time estimation (Fig. 2). Morphological analysis revealed mainly three types of aedeagus structural variations: (1) aedeagus with a single paramere

(Asp); (2) aedeagus with a bifurcated paramere (Abp); and (3) aedeagus with a pair of parameres (App).

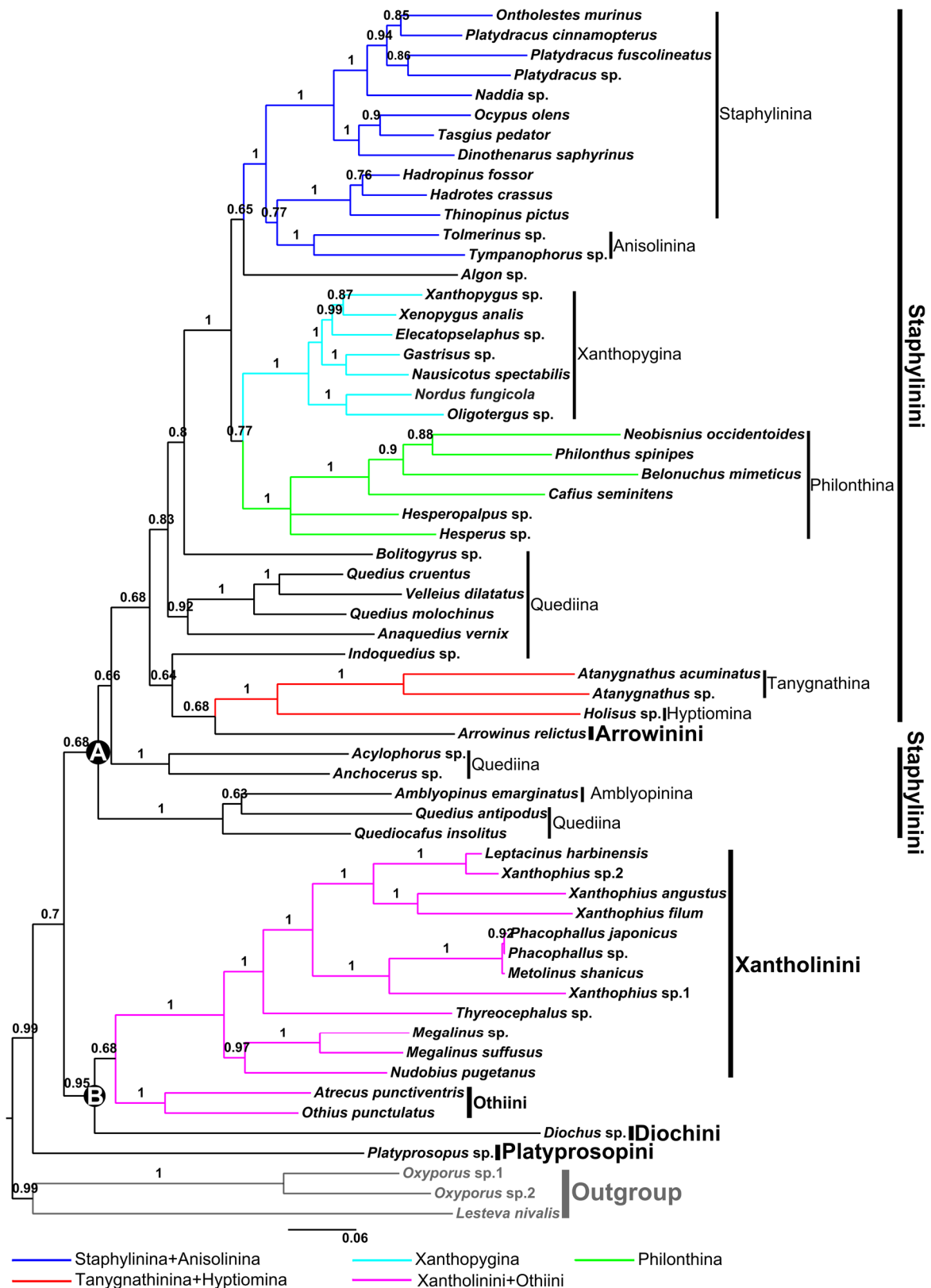


Figure 1. Bayesian phylogenetic tree for the partitioned combined analysis of four genes. Only posterior probabilities above 0.60 are shown. Colored branches represent the mainly monophyletic groups resolved in the phylogenetic inference. Verticle bars: thick bars denote the tribes of Staphylinini, thin bars the subtribes, grey bar the outgroup. The capital letters "A" and "B" refer to two main clades discussed in the text.

Table 2. Data set and the estimated models of sequence evolution by the Akaike information criterion (AIC).

Partition	Model (AIC)	P-Inv.	G-shape
COI_1st codon position*	T93+Γ+I	0.5	0.61
COI_2nd codon position*	HKY+Γ+I	0.67	0.62
COI_3rd codon position*	TN93+Γ	--	1.03
COI_total**	GTR+Γ+I	0.44	0.93
Wg_1st codon position*	JC+Γ	--	0.19
Wg_2nd codon position*	K2+Γ	--	0.23
Wg_3rd codon position*	T92+Γ	--	1.69
Wg_total**	T92+Γ+I	0.43	0.96
Tp_1st codon position*	GTR+Γ+I	0.47	0.77
Tp_2nd codon position*	GTR+Γ	--	0.25
Tp_3rd codon position*	K2+Γ+I	0.02	1.8
Tp_total**	T93+Γ+I	0.39	0.89
28S_total**	K2+Γ	--	0.22

*Codon partition

**The main partitions

Table 3. Summary of the Beast analysis for the age and nuclear substitution rates of important nodes from the concatenated sequence.

Main clade	Age (Mya)		Substitution rate	
	Mean	95% HPD*	Mean	95% HPD*
Staphylinina	176.11	161.38–190.78	2.31×10^{-3}	0.60×10^{-3} – 4.86×10^{-3}
Clade A	156.7	141.51–172.46	2.79×10^{-3}	1.16×10^{-3} – 5.20×10^{-3}
Clade B	154.43	135.97–172.79	2.32×10^{-3}	0.91×10^{-3} – 4.62×10^{-3}
Staphylinina+Anisolinina	93.39	77.73–110.37	1.63×10^{-3}	0.52×10^{-3} – 3.42×10^{-3}
Xanthopygina	56.85	41.2–74.45	1.50×10^{-3}	0.86×10^{-3} – 2.90×10^{-3}
Philonthina	87.86	71.95–105.56	2.70×10^{-3}	1.23×10^{-3} – 5.08×10^{-3}
Tanygnathina+Hyptiominina	97.23	70.69–122.1	2.34×10^{-3}	0.91×10^{-3} – 4.43×10^{-3}
Othiini	89.32	48.85–124.63	1.24×10^{-3}	0.53×10^{-3} – 2.57×10^{-3}
Xantholinini	110.05	91.96–129.93	4.24×10^{-3}	2.45×10^{-3} – 6.73×10^{-3}

*HPD represents the highest posterior density

Plotting three types of the aedeagus listed above on the phylogenetic tree (Fig. 2), we found at first that within Clade A, the aedeagus of the taxa in clade 1 were all Asp type (red arrow). This clade included mainly four sub-clades such as Staphylinina + Anisolinina, Xanthopygina, Philonthina and Tanygnathina + Hyptiominina and their divergence was estimated to begin at early Cretaceous (vertical dash line a). Second, clade 2 (including the genera *Anchocerus*, *Acylophorus*, *Anaquedius*, *Indoquedius*, *Velleius* and *Quedius*, these genera traditionally belong to the subtribe Quediina) and clade 3 (including the tribe Arrowinini and clade Tanygnathina + Hyptiominina) were all Abp type (black arrows), except for the tribe Arrowinini, the subtribe Tanygnathina and the genus *Quedius*; for these clades, Arrowinini was App type, whereas Tanygnathina and the genus *Quedius* were Asp type. Third, the sub-clades of Clade B were all App type (purple arrow), and the divergence time of this clade was estimated at about 154.43 Mya with a 95% confidence interval from 135.97 Mya to 172.79 Mya (vertical dash line b).

In Clade A, the morphological variations of the aedeagus along with the evolutionary times were as follows: initially, the aedeagus was Abp type at about early Cretaceous and then a transition to Asp type occurred during the middle to late Cretaceous (clade 2 in Fig. 2, black arrow 1); App type aedeagus changed directly to Asp type during early Cretaceous to early Paleogene (clade 3 in Fig. 2, black arrow 2). All genera in clade 1 have Asp type aedeagus. Within Clade B, the aedeagus was initially App type at about late Jurassic and then the double parameres were gradually shortened and ultimately disappeared completely at about late Quaternary.

With a perspective view on the general tendency of aedeagal paramere evolution, as shown in the phylogenetic tree (Fig. 2), we drew the following conclusion: in Clade A, from clade 3 to clade 2 and clade 1, aedeagal parameres changed

from paired to single; accompanied with the process of paramere changing, the number of terminal taxa (genera) were increasing gradually with active cladogenesis (especially so in clade 1). Some of the later-emerged genera were large ones and species-rich with hundreds and thousands of species (as *Philonthus* and so on). In Clade B, along with cladogenesis and new-taxon originating, aedeagal paramere evolution was seen to occur: here the paired parameres did not evolve into a single paramere but rather tended to decrease the lengths of parameres and median-lobe (penis itself). Obviously, either in Clade A or B, the aedeagus evolution was shown to occur with rove beetle cladogenesis.

3.3 The relationship between species richness and aedeagus morphological variation

Clades A and B (as shown in Figs 1–2), representing two clades with single paramere and paired parameres of aedeagus respectively. If we considered evolutionary time as starting point of comparison and plotted both PM index values (Y axis in Figs 3a, c) and the species numbers per selected genera (Y axis in Figs 3b, d) with cladogenesis time (from early to the most recent time in the phylogenetic tree, X axis in Fig. 3). An obvious and clear pattern appeared: along with the advancing of the evolutionary time, the variation scopes (the differences between the maximal and the minimal values at about the same time period) tended to increase, as shown by the dotted lines in Fig. 3. This pattern implied that speciation might be accompanied by modification and evolution of the aedeagus structures; diversity (species number and morphology) tended to increase along with the phylogenetic or evolutionary process.

In addition to variation scopes, we found that PM index values were increased along with phylogenetic diversification, which means that the parameres were changed to be shorter compared to the total aedeagus length. Similarly, along with PM index values increasing, the species numbers of most selected genera were increased along with the advancing of evolutionary time, especial those genera like *Platydracus*, *Ocypus*, *Xanthopygus*, *Philonthus*, *Acylophorus*, *Atanygnathus* in Clade A, and the *Leptacinus* in Clade B (Figs 3b, d). This implies that most rove beetle genera considered here tended to be more diverse with more active cladogenesis and morphological diversification, at least in aedeagus structures.

These result offered us a primary but meaningful pattern: this could tell us that, along with rove beetle evolution, aedeagus morphology changed to be more diverse in different genus-level taxa and the species numbers of a single genus exhibited larger differences among all those extant genera, no matter they originated in very earlier time or somehow later near recent time. Some genera changed to be larger with a large number of species. This was a consequence of cladogenesis/speciation minus extinctions. This pattern gave us at least one of many aspects of Staphylininae phylogenetic history, which might be correlated with a certain kind of mechanism of aedeagus modification.

4 Discussion

Beetles represent one of the most diversified lineages on the earth and their extraordinary diversity has long fascinated evolutionary biologists (Crowson, 1960; Farrell, 1998; Hunt *et al.*, 2007; Sota & Nagata, 2008; Lawrence *et al.*, 2011). Many excellent advances have been made in recognizing large-scale patterns of phytophagous beetle species diversity in last two decade, such as the diversification of phytophagous insect lineages might be driven by co-radiations with angiosperms (Farrell, 1998; Wilf *et al.*, 2000), and/or by repeated radiation on a pre-existing diverse resource, rather than by ancient host associations (Gómez-Zurita *et al.*, 2007); or linked to mutualisms with microbes (Janson *et al.*, 2008); or promoted by the repeated climate-linked host shifts (Winkler *et al.*, 2009). However, these hypotheses were not able to explain the extraordinary diversity of non-phytophagous beetles (e.g., rove beetles and carrion beetles).

According to well-known theoretical hypotheses, such as sexual selection and the related mechanism of speciation (Eberhard, 1985; Arnqvist & Danielsson, 1999; Hosken & Stockley, 2004; House & Simmons, 2005; Wenninger & Averill, 2006; Ritchie, 2007; Eberhard, 2010), the extreme diversity of genital morphology might be an important factor contributing to current beetle diversity. Thus, elucidating the evolutionary processes underlying aedeagal morphological diversity has the potential of providing tremendous insight into understanding the species diversity of rove beetles. By identifying the pattern of major character transitions throughout the evolutionary history of a group, we can begin to establish a phylogenetically informed hypothesis concerning the processes leading to these patterns (Matocq *et al.*, 2007). In this study, we used mitochondrial and nuclear loci whose rates of molecular evolution are, in combination, informative at the range of evolutionary depths that encompass the history of the subfamily Staphylininae. We used these markers in conjunction with Bayesian and maximum likelihood methods, two phylogenetic analyses frequently used to estimate evolutionary relationships (Elven *et al.*, 2010). Our estimation of phylogenetic relationships of Staphylininae adds new data and views to the ongoing study of evolutionary affinities of the taxon and may offer penetrating ideas to the field.

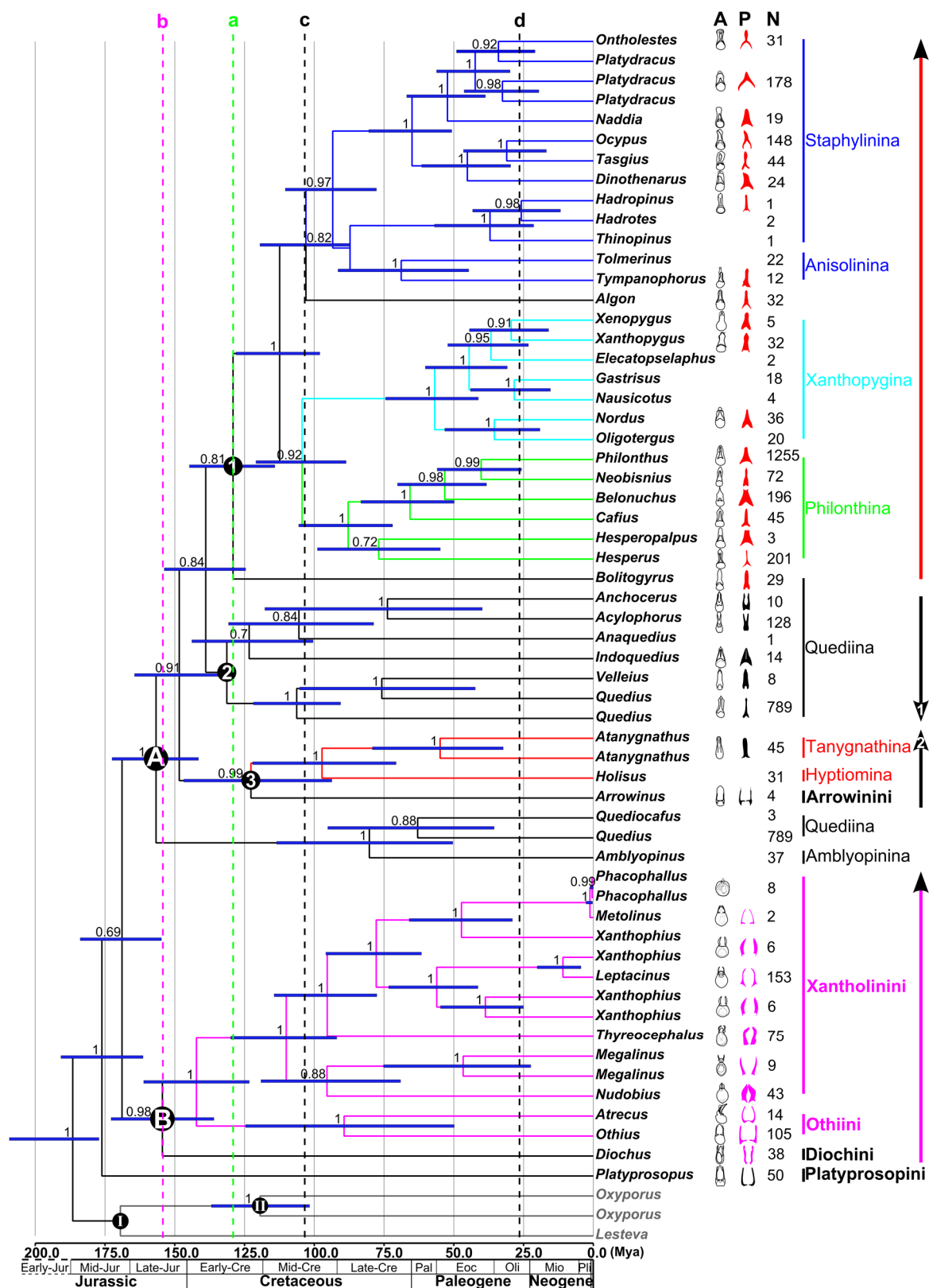


Figure 2. Figure 2. Phylogeny of the subfamily Staphylininae with divergence time estimates based on the concatenated sequence. Blue bars at each node show 95% highest posterior density interval for the main nodes. Colored branches and circled capital letters are as in Figure 1. Circled numbers refer to three main sub-clades within Clade A discussed in text. Circled roman letters represent the calibration points. Capital letter 'A', 'P' and 'N' represent aedeagus, paramere and species number of each corresponding genus respectively. Colored arrows refer to phylogenetic patterns of aedeagus morphology discussed in text. Dot lines with lower case letters refer to divergence times discussed in text. The abbreviation of geological ages are as follows: Jur—Jurassic; Cre—Cretaceous; Pal—Paleocene; Eoc—Eocene; Oli—Oligocene; Mio—Miocene; Pli—Pliocene.

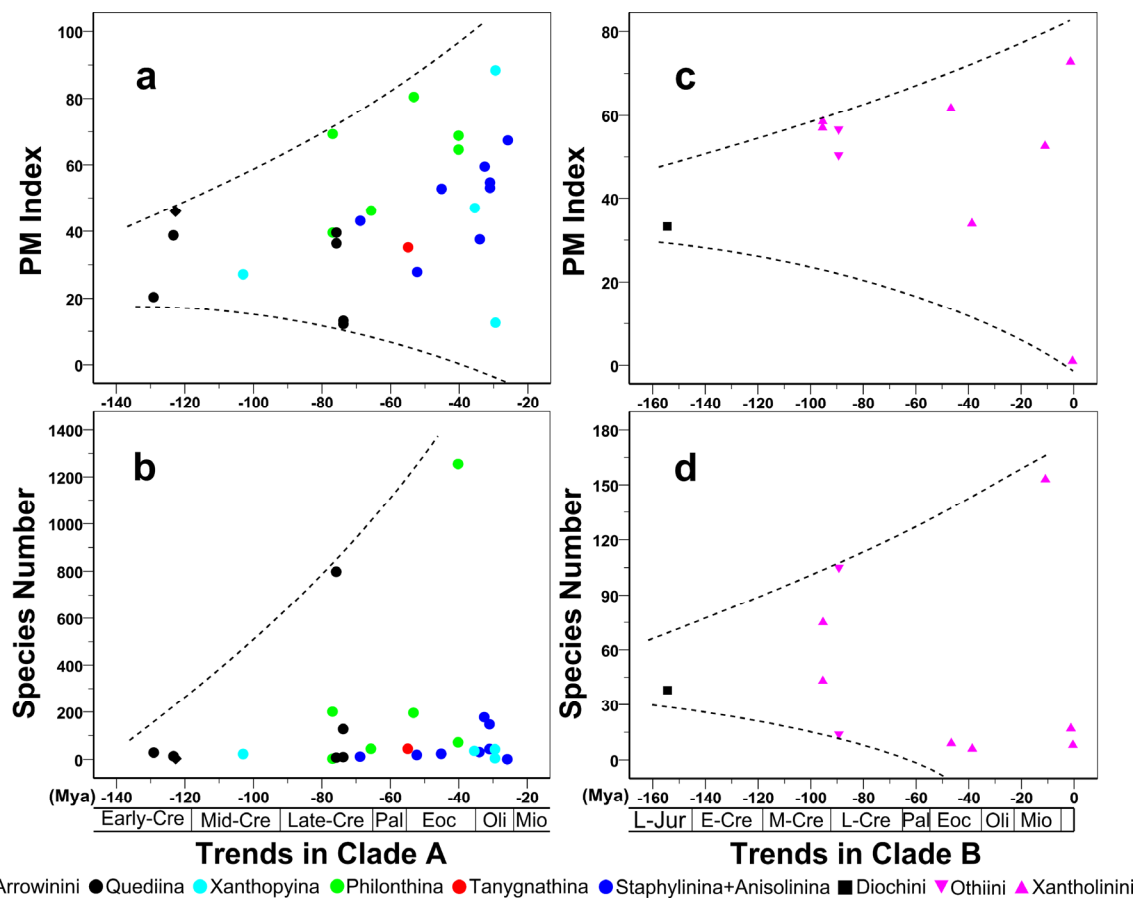


Figure 3. Plotting Paramere-to-Median-lobe Index (PM Index) and the number of species of the selected genera (Y axis) with the divergence time (X axis) estimated. PM Index variations along with divergence time (a, c); species number variations along with evolutionary time (b, d). The abbreviation of geological ages are as follows: Jur—Jurassic; Cre—Cretaceous; Pal—Paleocene; Eoc—Eocene; Oli—Oligocene; Mio—Miocene; Pli—Pliocene.

The molecular clock calculation on the Bayesian hypothesis of Staphylininae phylogeny suggests that most genera of the subfamily originated from middle Cretaceous to late Paleogene (between dash line c and dash line d in Fig. 2). This result is consistent with many previous studies on age estimation of other beetle groups (Gómez-Zurita *et al.*, 2007; Hunt *et al.*, 2007; Ge *et al.*, 2011). Within Clade A, the length ratios of paramere/aedeagus were decreased in general along with the evolution time, and the later the origin time, the greater the variation in scopes (Figs 2–3). This large variation in the scopes of aedeagus morphology may be helpful for the taxon to get advantage in sexual selection, which has a reputation as a major cause of speciation (Ritchie, 2007; Reinhardt, 2010). The species number of each corresponding genus, along with evolution time, was basically from less to more, and the later the origin time, the greater the species richness, especially during late Cretaceous to Eocene epoch (Fig. 2). This diversity increase may correlate with the Paleocene-Eocene adaptive radiation of those lineages survived until Cretaceous as many groups of organisms (Labandeira *et al.*, 2002; McKenna & Farrell, 2006). The evolutionary trends of aedeagus morphology and species richness within Clade B were basically the same as those of Clade A (Figs 2–3). However, the genus *Phacophallus* possessed an aedeagus with no paramere, which originated from about late Quaternary. This may indicate that the evolutionary rate of taxa in clade Xantholinini was accelerated during the Quaternary period (the last 1.8 million years); this period is characterized by multiple climatic changes in the form of glacial-interglacial transitions that operated at the 100,000 year time scale and appreciably influenced evolutionary patterns in organisms (Barnosky, 2005).

The phylogenetic hypothesis generated herein allows us to hypothesize a simplistic development model for the range of aedeagus morphological diversity observed within the subfamily Staphylininae (Fig. 2). Obviously, the ancestral form of the aedeagus in the subfamily possessed aedeagus with the App type, and then it possibly evolved along two different evolutionary pathways. One pathway is that the aedeagus was always with double parameres during the evolutionary process, and the length of the paramere gradually shortened along with evolutionary time until it completely disappeared, just like taxa in Clade B. The other evolutionary pathway could be divided into two steps. The first possible scenario is that, along

with the evolutionary time, the double parameres became fused at the base of each paramere and then transitioned into a single paramere, just like taxa in sub-clade 2 and sub-clade 3 of Clade A. The second step is that the single paramere gradually shortened along with evolutionary time, just like taxa in sub-clade 1 of Clade A.

Funding This study was supported by the National Natural Science Foundation of China (31472036, 31272358), the Ministry of Science and Technology of China (2015FY210300) and a grant from the Key Laboratory of the Zoological Systematics and Evolution of CAS (Y229YX5105).

Acknowledgements We thank Ms. Y.L.Z. Zhou, Dr. L. Li, Dr. X.Y. Li and Dr. Z. Yang for collecting and identifying valuable specimens used in this study.

References

- Arnqvist, G. 1997. The evolution of animal genitalia: distinguishing between hypotheses by single species studies. *Biological Journal of the Linnean Society*, 60: 365–379.
- Arnqvist, G. 1998. Comparative evidence for the evolution of genitalia by sexual selection. *Nature*, 393: 784–786.
- Arnqvist, G., Danielsson, I. 1999. Copulatory behavior, genital morphology, and male fertilization success in water striders. *Evolution*, 53: 147–156.
- Barnosky, A.D. 2005. Effects of Quaternary climatic change on speciation in mammals. *Journal of Mammalian Evolution*, 12: 247–264.
- Bouchard, P., Grebennikov, V.V., Smith, A.B.T., Douglas, H. 2009. Biodiversity of Coleoptera. In: Foottit, R.G., Adler, P.H. (eds), *Insect Biodiversity: Science and Society*. Wiley-Blackwell, Oxford, Chichester and Hoboken. pp. 265–301.
- Cai, C., Huang, D. 2010. Current knowledge on Jurassic staphylinids of China (Insecta, Coleoptera). *Earth Science Frontiers*, 17: 151–153.
- Chatzimanolis, S., Cohen, I.M., Schomann, A., Solodovnikov, A. 2010. Molecular phylogeny of the mega-diverse rove beetle tribe Staphylinini (Insecta, Coleoptera, Staphylinidae). *Zoologica Scripta*, 39: 436–449.
- Crowson, R.A. 1960. The phylogeny of Coleoptera. *Annual Review of Entomology Palo Alto*, 5: 111–134.
- Drummond, A.J., Ho, S.Y.W., Phillips, M.J., Rambaut, A. 2006. Relaxed phylogenetics and dating with confidence. *Plos Biology*, 4: 699–710.
- Drummond, A.J., Rambaut, A. 2007. BEAST: Bayesian evolutionary analysis by sampling trees. *Bmc Evolutionary Biology*, 7: 214.
- Eberhard, W. 2010. Evolution of genitalia: theories, evidence, and new directions. *Genetica*, 138: 5–18.
- Eberhard, W.G. 1985. *Sexual Selection and Animal Genitalia*. Harvard University Press, Cambridge, Massachusetts and London.
- Eberhard, W.G., Huber, B.A., Lucas, R.S.R., Briceno, R.D., Salas, I., Rodriguez, V. 1998. One size fits all? Relationships between the size and degree of variation in genitalia and other body parts in twenty species of insects and spiders. *Evolution*, 52: 415–431.
- Edwards, R. 1993. Entomological and Mammalogical Perspectives on Genital Differentiation. *Trends in Ecology and Evolution*, 8: 406–409.
- Elven, H., Bachmann, L., Gusarov, V.I. 2010. Phylogeny of the tribe Athetini (Coleoptera: Staphylinidae) inferred from mitochondrial and nuclear sequence data. *Molecular Phylogenetics and Evolution*, 57: 84–100.
- Engel, M.S., Grimaldi, D.A. 2004. New light shed on the oldest insect. *Nature*, 427: 627–630.
- Farrell, B.D. 1998. "Inordinate fondness" explained: Why are there so many beetles? *Science*, 281: 555–559.
- Ge, D.Y., Chesters, D., Gomez-Zurita, J., Zhang, L.J., Yang, X.K., Vogler, A.P. 2011. Anti-predator defence drives parallel morphological evolution in flea beetles. *Proceedings of the Royal Society B-Biological Sciences*, 278: 2133–2141.
- Gillespie, J., Cannone, J., Gutell, R., Cognato, A. 2004. A secondary structural model of the 28S rRNA expansion segments D2 and D3 from rootworms and related leaf beetles (Coleoptera : Chrysomelidae; Galerucinae). *Insect Molecular Biology*, 13: 495–518.
- Gómez-Zurita, J., Hunt, T., Kopliku, F., Vogler, A.P. 2007. Recalibrated tree of leaf beetles (Chrysomelidae) indicates independent diversification of angiosperms and their insect herbivores. *Plos One*, 2: e360.
- Grebennikov, V.V., Newton, A.F. 2009. Good-bye Scydmaenidae, or why the ant-like stone beetles should become megadiverse Staphylinidae sensu latissimo (Coleoptera). *European Journal of Entomology*, 106: 275–301.
- Grove, S.J., Stork, N.E. 2000. An inordinate fondness for beetles. *Invertebrate Taxonomy*, 14: 733–739.
- Guindon, S., Gascuel, O. 2003. A simple, fast, and accurate algorithm to estimate large phylogenies by maximum likelihood. *Systematic Biology*, 52: 696–704.
- Herman, L.H. 2001. Catalog of the Staphylinidae (Insecta: Coleoptera): 1758 to the end of the second millennium. VII. Bibliography and index. *Bulletin of the American Museum of Natural History*, 265(Part 7): 3841–4218.
- Higgins, D.G., Larkin, M.A., Blackshields, G., Brown, N.P., Chenna, R., McGettigan, P.A., McWilliam, H., Valentin, F., Wallace, I.M., Wilm, A., Lopez, R., Thompson, J.D., Gibson, T.J. 2007. Clustal W and clustal X version 2.0. *Bioinformatics*, 23: 2947–2948.
- Hosken, D.J., Stockley, P. 2004. Sexual selection and genital evolution. *Trends in Ecology and Evolution*, 19: 87–93.

- Ho, S.Y.W. 2007. Calibrating molecular estimates of substitution rates and divergence times in birds. *Journal of Avian Biology*, 38: 409–414.
- House, C.M., Simmons, L.W. 2005. The evolution of male genitalia: patterns of genetic variation and covariation in the genital sclerites of the dung beetle *Onthophagus taurus*. *Journal of Evolutionary Biology*, 18: 1281–1292.
- Hunt, T., Bergsten, J., Levkanicova, Z., Papadopoulou, A., St. John, O., Wild, R., Hammond, P.M., Ahrens, D., Balke, M., Caterino, M.S., Gómez-Zurita, J., Ribera, I., Barraclough, T.G., Bocakova, M., Bocak, L., Vogler, A.P. 2007. A comprehensive phylogeny of beetles reveals the evolutionary origins of a superradiation. *Science*, 318: 1913–1916.
- Ikeda, H., Nishikawa, M., Sota, T. 2012. Loss of flight promotes beetle diversification. *Nature Communications*, 3: 648.
- Janson, E.M., Stireman, J.O., Singer, M.S., Abbot, P. 2008. Phytophagous insect-microbe mutualisms and adaptive evolutionary diversification. *Evolution*, 62: 997–1012.
- Labandeira, C.C., Johnson, K.R., Wilf, P. 2002. Impact of the terminal Cretaceous event on plant-insect associations. *Proceedings of the National Academy of Sciences of the United States of America*, 99: 2061–2066.
- Lawrence, J.F., Slipinski, A., Seago, A.E., Thayer, M.K., Newton, A.F., Marvaldi, A.E. 2011. Phylogeny of the Coleoptera based on morphological characters of adults and larvae. *Annales Zoologici*, 61: 1–217.
- Matocq, M.D., Shurtliff, Q.R., Feldman, C.R. 2007. Phylogenetics of the woodrat genus *Neotoma* (Rodentia: Muridae): Implications for the evolution of phenotypic variation in male external genitalia. *Molecular Phylogenetics and Evolution*, 42: 637–652.
- McKenna, D.D., Farrell, B.D. 2006. Tropical forests are both evolutionary cradles and museums of leaf beetle diversity. *Proceedings of the National Academy of Sciences of the United States of America*, 103: 10947–10951.
- Mendez, V., Cordoba-Aguilar, A. 2004. Sexual selection and animal genitalia. *Trends in Ecology and Evolution*, 19: 224–225.
- Newton, A.F., Thayer, M.K. 1992. Current classification and family-group names in Staphyliniformia (Coleoptera). *Fieldiana Zoology*, 67: 1–92.
- Novotny, V., Drozd, P., Miller, S.E., Kulfan, M., Janda, M., Basset, Y., Weiblen, G.D. 2006. Why are there so many species of herbivorous insects in tropical rainforests? *Science*, 313: 1115–1118.
- Posada, D., Crandall, K.A. 1998. MODELTEST: testing the model of DNA substitution. *Bioinformatics*, 14: 817–818.
- Rambaut, A. 2002. Se-Al: Sequence Alignment Editor. Version 2.0 Available from <http://tree.bio.ed.ac.uk/software/seal/> (accessed 28 July, 2012)
- Rambaut, A. 2009. FigTree 1.3. Available from <http://tree.bio.ed.ac.uk/software/figtree/> (accessed 12 Dec 2016)
- Rambaut, A., Drummond, A.J. 2007. Tracer v1.5. Available from <http://beast.bio.ed.ac.uk/Tracer> (accessed 12 Dec 2016)
- Reinhardt, K. 2010. Natural selection and genital variation: a role for the environment, parasites and sperm ageing? *Genetica*, 138: 119–127.
- Ritchie, M.G. 2007. Sexual selection and speciation. *Annual Review of Ecology Evolution and Systematics*, 38: 79–102.
- Roff, D.A. 1990. The evolution of flightlessness in insects. *Ecological Monographs*, 60: 389–421.
- Ronquist, F., Huelsenbeck, J.P. 2003. MrBayes 3: Bayesian phylogenetic inference under mixed models. *Bioinformatics*, 19: 1572–1574.
- Simmons, L.W., Ridsdill-Smith, T.J. 2011. Reproductive competition and its impact on the evolution and ecology of dung beetles. In: Simmons, L.W., Ridsdill-Smith, T.J. (eds), *Ecology and Evolution of Dung Beetles*. Wiley-Blackwell, Oxford, Chichester and Hoboken. pp. 1–20.
- Solodovnikov, A.Y., Newton, A.F. 2005. Phylogenetic placement of Arrowinini trib. n. within the subfamily Staphylininae (Coleoptera: Staphylinidae), with revision of the relict South African genus *Arrowinus* and description of its larva. *Systematic Entomology*, 30: 398–441.
- Sota, T., Nagata, N. 2008. Diversification in a fluctuating island setting: rapid radiation of Ohomopterus ground beetles in the Japanese Islands. *Philosophical transactions of the Royal Society B*, 363: 3377–3390.
- Tamura, K., Peterson, D., Peterson, N., Stecher, G., Nei, M., Kumar, S. 2011. MEGA5: Molecular evolutionary genetics analysis using maximum likelihood, evolutionary distance, and maximum parsimony methods. *Molecular Biology and Evolution*, 28: 2731–2739.
- Wenninger, E.J., Averill, A.L. 2006. Influence of body and genital morphology on relative male fertilization success in oriental beetle. *Behavioral Ecology*, 17: 656–663.
- Wilf, P., Labandeira, C.C., Kress, W.J., Staines, C.L., Windsor, D.M., Allen, A.L., Johnson, K.R. 2000. Timing the radiations of leaf beetles: hispines on gingers from latest Cretaceous to Recent. *Science*, 289: 291–294.
- Winkler, I.S., Mitter, C., Scheffer, S.J. 2009. Repeated climate-linked host shifts have promoted diversification in a temperate clade of leaf-mining flies. *Proceedings of the National Academy of Sciences of the United States of America*, 106: 18103–18108.
- Yue, Y.L., Ren, D., Solodovnikov, A. 2011. The oldest fossil species of the rove beetle subfamily Oxyporinae (Coleoptera: Staphylinidae) from the Early Cretaceous (Yixian Formation, China) and its phylogenetic significance. *Journal of Systematic Palaeontology*, 9: 467–471.
- Zhang, X., Zhou, H.Z. 2013. How old are the rove beetles (Insecta: Coleoptera: Staphylinidae) and their lineages? Seeking an answer with DNA. *Zoological Science*, 30: 490–501.

Supplementary material

Table S1. Species of the subfamily Staphylininae and related taxa included in the molecular analysis, and accession numbers of the corresponding individual sequence.

Subfamily	Tribe/Subtribe	Species	COI	Wingless	28S	Tp
Staphylininae	Arrowinini	<i>Arrowinus relictus</i>	GU377361	GU377462	-	GU377411
	Diochini	<i>Diochus</i> sp.	GU377370	GU377471	GU377325	GU377420
	Othiini	<i>Atrecus punctiventris</i>	GU377365	GU377466	GU377321	GU377415
		<i>Othius punctulatus</i>	GU377385	GU377487	GU377339	GU377436
	Platyprosopini	<i>Platyprosopus</i> sp.	GU377391	GU377493	GU377344	GU377442
	Staphylinini/Amblyopinina	<i>Amblyopinus emarginatus</i>	GU377357	GU377458	GU377315	GU377407
	Staphylinini/Anisolinina	<i>Tolmerinus</i> sp.	GU377360	GU377461	GU377317	GU377410
		<i>Tympanophorus</i> sp.	GU377401	GU377503	GU377351	GU377452
	Staphylinini/Hyptiomina	<i>Holius</i> sp.	GU377375	GU377477	GU377331	GU377426
	Staphylinini/Philonthina	<i>Belonuchus mimeticus</i>	GU377366	GU377467	GU377322	GU377416
		<i>Cafius seminitens</i>	GU377368	GU377469	-	GU377418
		<i>Hesperopalpus</i> sp.	GU377388	GU377490	GU377341	GU377439
		<i>Hesperus</i> sp.	GU377374	GU377476	GU377330	GU377425
		<i>Neobisnius occidentoides</i>	GU377379	GU377481	-	GU377430
		<i>Philonthus spinipes</i>	JX878801	JX878748	JX878695	GU377438
		<i>Acylophorus</i> sp.	GU377355	GU377456	-	GU377405
		<i>Anaquedius vernix</i>	GU377358	GU377459	GU377316	GU377408
		<i>Anchocerus</i> sp.	GU377359	GU377460	-	GU377409
		<i>Bolitogyrus</i> sp.	GU377367	GU377468	GU377323	GU377417
	Staphylinini/Quediina	<i>Indoquedius</i> sp.	GU377376	GU377478	-	GU377427
		<i>Quediocafus insolitus</i>	GU377392	GU377494	GU377345	GU377443
		<i>Quedius antipodus</i>	GU377393	GU377495	GU377346	GU377444
		<i>Quedius cruentus</i>	GU377394	GU377496	GU377347	GU377445
		<i>Quedius molochinus</i>	GU377396	GU377498	GU377348	GU377447
		<i>Velleius dilatatus</i>	GU377402	GU377504	GU377352	GU377453
		<i>Dinothenarus saphyrinus</i>	GU377369	GU377470	GU377324	GU377419
		<i>Hadropinus fossor</i>	GU380341	GU377474	GU377328	GU377423
		<i>Hadrotes crassus</i>	GU377373	GU377475	GU377329	GU377424
		<i>Naddia</i> sp.	GU377377	GU377479	GU377332	GU377428
	Staphylinini/Staphylinina	<i>Ocypus olens</i>	GU377382	GU377484	GU377336	GU377433
		<i>Ontholestes murinus</i>	GU377384	GU377486	GU377338	GU377435
		<i>Platydracus cinnamopterus</i>	GU377389	GU377491	GU377342	GU377440
		<i>Platydracus fuscolineatus</i>	JX878802	JX878749	JX878696	-
		<i>Platydracus</i> sp.	GU377390	GU377492	GU377343	GU377441
		<i>Tasgius pedator</i>	GU377399	GU377501	GU377349	GU377450
		<i>Thinopinus pictus</i>	GU377400	GU377502	GU377350	GU377451
		<i>Atanygnathus acuminatus</i>	GU377363	GU377464	GU377319	GU377413
		<i>Atanygnathus</i> sp.	GU377364	GU377465	GU377320	GU377414
	Staphylinini/Xanthopygina	<i>Algon</i> sp.	GU377356	GU377457	GU377314	GU377406
		<i>Elecatopselaphus</i> sp.	GU377371	GU377472	GU377326	GU377421
		<i>Gastrisus</i> sp.	GU377372	GU377473	GU377327	GU377422
		<i>Nausicotus spectabilis</i>	GU377378	GU377480	GU377333	GU377429
		<i>Nordus fungicola</i>	GU377380	GU377482	GU377334	GU377431
		<i>Oligotergus</i> sp.	GU377383	GU377485	GU377337	GU377434

Table S1 (continued)

Subfamily	Tribe/Subtribe	Species	COI	Wingless	28S	Tp
	Xantholinini	<i>Xanthopygus</i> sp.	GU377403	GU377505	GU377353	GU377454
		<i>Xenopygus analis</i>	GU377404	GU377506	GU377354	GU377455
		<i>Leptacinus harbinensis</i>	JX878803	JX878750	JX878697	*
		<i>Megalinus</i> sp.	JX878804	JX878751	JX878698	-
		<i>Megalinus suffusus</i>	JX878805	JX878752	JX878699	-
		<i>Metolinus shanicus</i>	JX878806	JX878753	JX878700	*
		<i>Nudobius pugetanus</i>	GU377381	GU377483	GU377335	GU377432
		<i>Phacophallus japonicus</i>	JX878807	JX878754	JX878701	-
		<i>Phacophallus</i> sp.	JX878808	JX878755	JX878702	-
		<i>Thyrecephalus</i> sp.	JX878809	JX878756	JX878703	-
		<i>Xanthophius angustus</i>	JX878810	JX878757	JX878704	*
		<i>Xanthophius filum</i>	JX878811	JX878758	JX878705	-
		<i>Xanthophius</i> sp.1	JX878812	JX878759	JX878706	-
		<i>Xanthophius</i> sp.2	JX878813	JX878760	JX878707	-
Oxyporinae		<i>Oxyporus</i> sp.1	JX878817	JX878764	JX878711	*
		<i>Oxyporus</i> sp.2	JX878818	JX878765	JX878712	*
Omalinae		<i>Lesteva nivalis</i>	JX878822	JX878769	JX878716	*

Table S2. Primers used to amplify the sequences studied.

Gene	Primer name	F/R	Sequence (5'–3')	References
mtDNA				
COI	Jerry	F	CAACATTTATTTTGATTTTTTGG	Simon <i>et al.</i> , 1994
	Pat	R	TCCAATGCACTAATCTGCCATATTA	Simon <i>et al.</i> , 1994
Nuclear				
Wingless	Wg550	F	ATGCGTCAGGARTGYAARTGYCAYGGYATGTC	Wild & Maddison, 2008
	Wg578	F	TGCCANGTGAARACYTGCTGGATG	Ward & Downie, 2005
	WgABR	R	ACYTCGCAGCACCARTGGAA	Abouheif & Wray, 2002
	WgABRZ	R	CACTTNACYTCRCARCACCARTG	Wild & Maddison, 2008
Tp	TP643	F	GACGATTGGAARTCNAARGARATG	Wild & Maddison, 2008
	TP675	F	GAGGACCAAGCNGAYACNGTDGGTTGTTG	Wild & Maddison, 2008
	TP919	R	GTCTCTTTGCGTYTTRTTRTADATYTTYTC	Wild & Maddison, 2008
	TP932	R	GGWCCDGCATCDATDGCCCA	Wild & Maddison, 2008
28S	NFL184-21	F	ACCCGCTGAAYTTAAGCATAT	Vanderauwera <i>et al.</i> , 1994
	LS1041	R	TACGGACRTCCATCAGGGTTTCCCCTGACTTC	Maddison, 2008

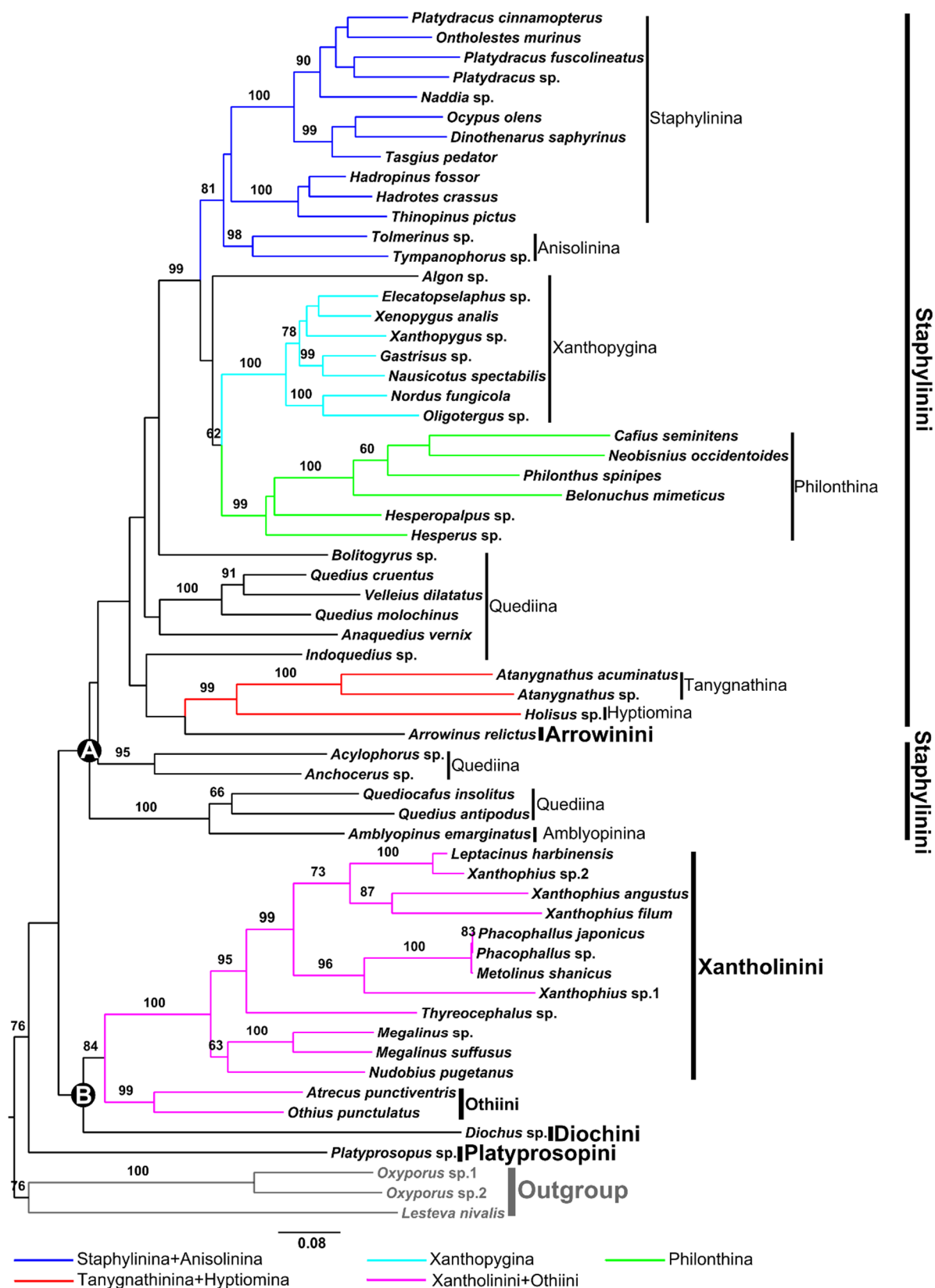


Figure S3. Maximum likelihood phylogenetic tree for the partitioned combined analysis of four genes. Only bootstrap values above 60 are shown. Colored branches represent the mainly monophyletic groups resolved in the phylogenetic inference. Black bars represent the suprageneric taxa of the subfamily Staphylininae: thick bars denote tribes; thin bars denote subtribes of Staphylinini. Grey bars represent the outgroup. Circled capital letters “A” and “B” refer to two main clades discussed in the text.